

## LA-UR-19-21297

Approved for public release; distribution is unlimited.

Title: FY 18 Summary Report on the Technology Transfer Work Package for the Northstar Mo99 Production Project

Author(s): Woloshun, Keith Albert

Intended for: Report

Issued: 2019-02-20

---

**Disclaimer:**

Los Alamos National Laboratory, an affirmative action/equal opportunity employer, is operated by Triad National Security, LLC for the National Nuclear Security Administration of U.S. Department of Energy under contract 89233218CNA000001. By approving this article, the publisher recognizes that the U.S. Government retains nonexclusive, royalty-free license to publish or reproduce the published form of this contribution, or to allow others to do so, for U.S. Government purposes. Los Alamos National Laboratory requests that the publisher identify this article as work performed under the auspices of the U.S. Department of Energy. Los Alamos National Laboratory strongly supports academic freedom and a researcher's right to publish; as an institution, however, the Laboratory does not endorse the viewpoint of a publication or guarantee its technical correctness.

# **FY 18 Summary Report on the Technology Transfer Work Package for the Northstar Mo99 Production Project**

Keith Woloshun

Los Alamos National Laboratory

2/4/2019

## **Introduction**

In FY18, Northstar began in earnest to transition from concept and process development to construction of a production facility for the conversion of Mo100 to Mo99 using an electron beam. Facility layouts comprised of 8 target stations were developed at LANL in 2014. The plan for production at that time was to use linear electron accelerators. Things have evolved since then, of course. Major changes include the switch to rhodotrons as the electron source and the initial plant scope reduced to a single target station.

In order for LANL to assist Northstar in achieving their production goal, the main work package for LANL in FY18 was termed Technology Transfer. This has evolved beyond transferring knowledge and information to assisting in the new plant design. Progress was significantly delayed because Northstar did not provide a point-of-contact until mid-year, at which point James McCarter was hired. This year-end report will detail the work done in support of the Northstar facility.

## **Shielding Analysis and Plant Layout Schemes**

The original intent was to have linear accelerators on the ground floor, with all services, including the helium cooling systems and the hot cell for target removal and insertion on an upper level, on top of the shielding. There were 2 accelerators per target for a 2-sided irradiation scheme. A cross-sectional view is shown in Figure 1.

Northstar has made 2 significant design changes. First, rhodotrons were selected as the electron source. The rhodotrons are 10 foot diameter machines. Second, the vertical insertion, with all the helium and target handling equipment on top of the shielding, is abandoned in preference to a horizontal target insertion with all supporting equipment on the ground floor.

The first order of business for Northstar is to determine the footprint of the facility and a general scheme of the layout so that their Architect and Engineering (A&E) can design the building. Northstar proposed some shielding layouts that were evaluated using MXNPX neutronics code by LANL for shielding adequacy (Figure 2). The large circle surrounding the target position is local neutron shielding (layered borated poly and steel). Shielding analysis results are shown in Figure 3 for 8 foot thick high density concrete shielding. A major driver in the design is the desire to be able to do maintenance and repairs on one rhodotron while the other is operating, hence the shield wall between the rhodotrons. A second analysis was done, shown in Figure 4. This indicates significant streaming through the beam pipe

penetration in the shield wall. A beam plug during maintenance will be required here, as well as minimizing the diameter of the wall penetration.

Subsequently, many configurations have been evaluated and now suitable solutions have been established for both high density and low density concrete. Many details remain to be resolved.

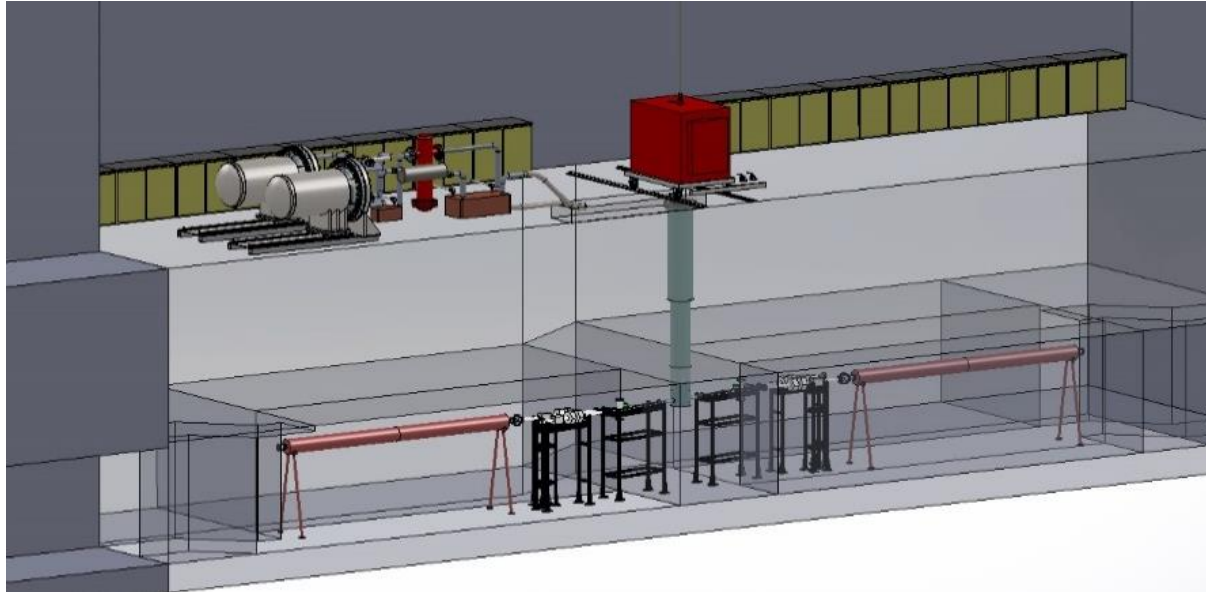


Figure 1. Linear accelerator driven production facility cross-sectional view, with vertical target insertion.

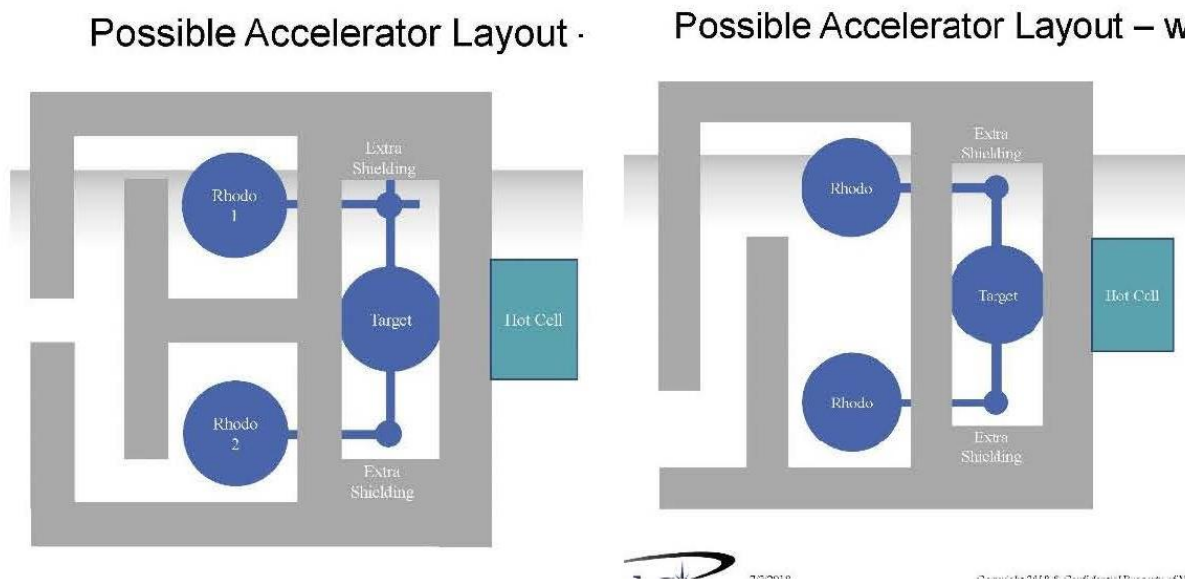
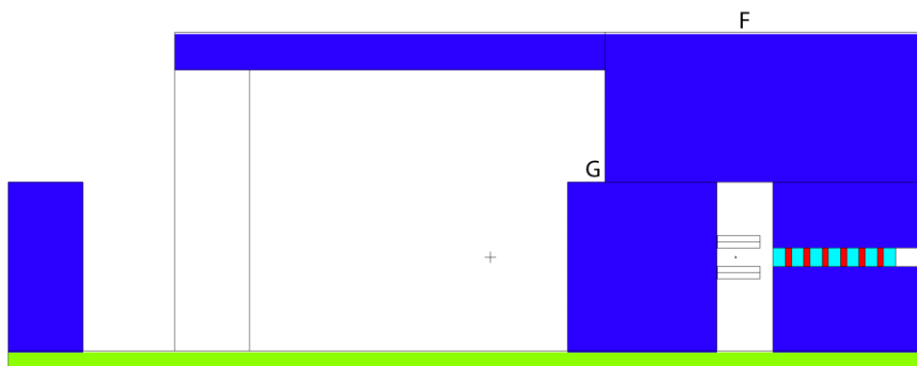
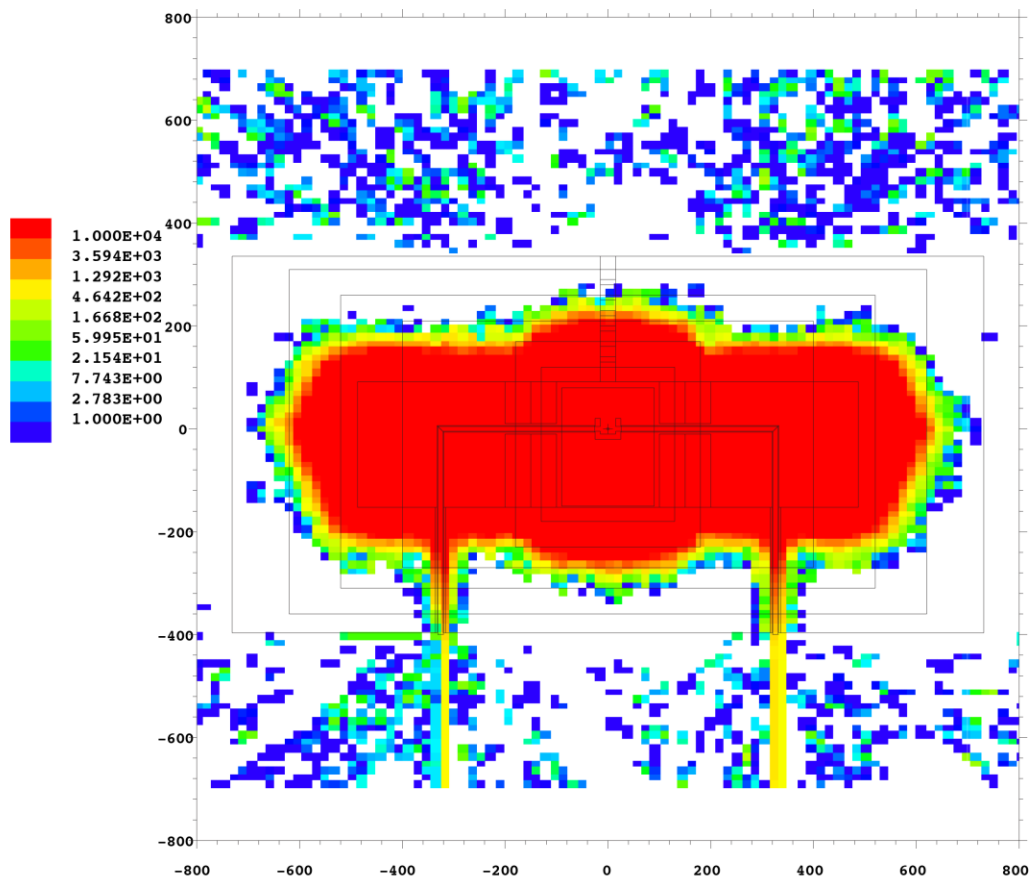
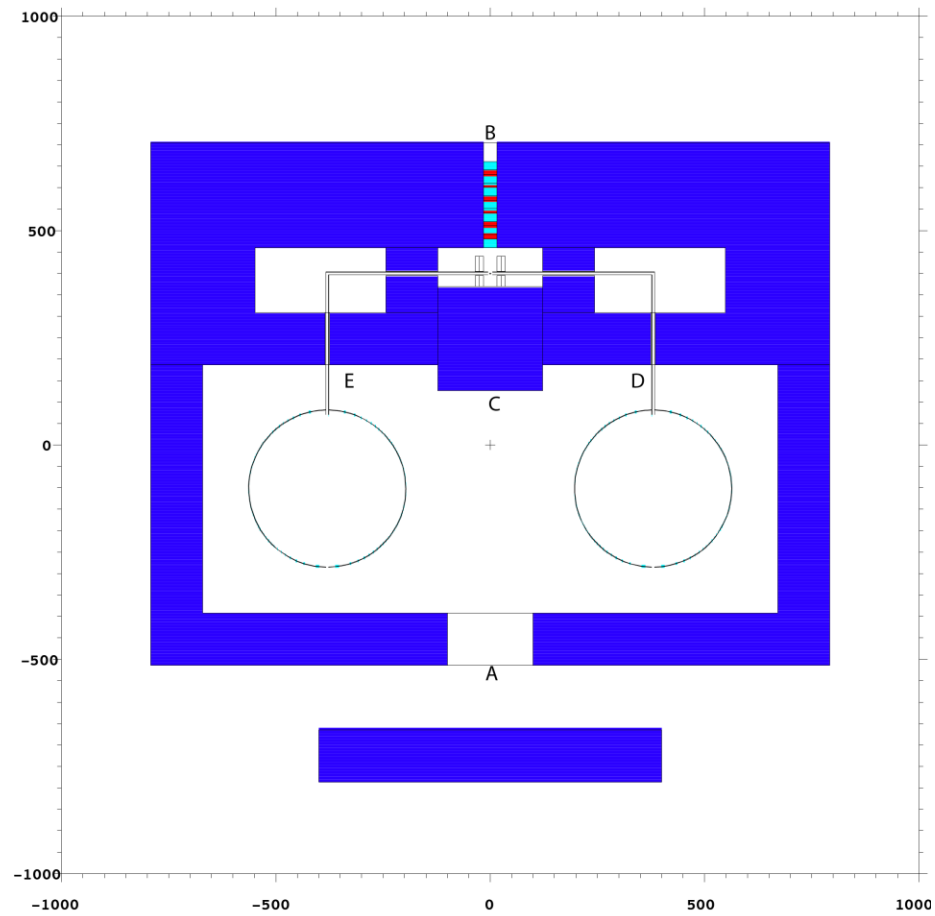


Figure 2. Optional shielding layouts proposed by Northstar.





Spot	Two sided mrem/h	One sided mrem/h
A	0.7	0.4
B	0.3	0.1
C	0.6	0.3
D	25	20
E	25	1
F	<0.1	<0.1
G	3-4	3

Figure 3. MCNPX Shielding analysis results. Top image shows a neutron flux map. The following figures and table show the dose rate at various locations for single and double sided irradiation.

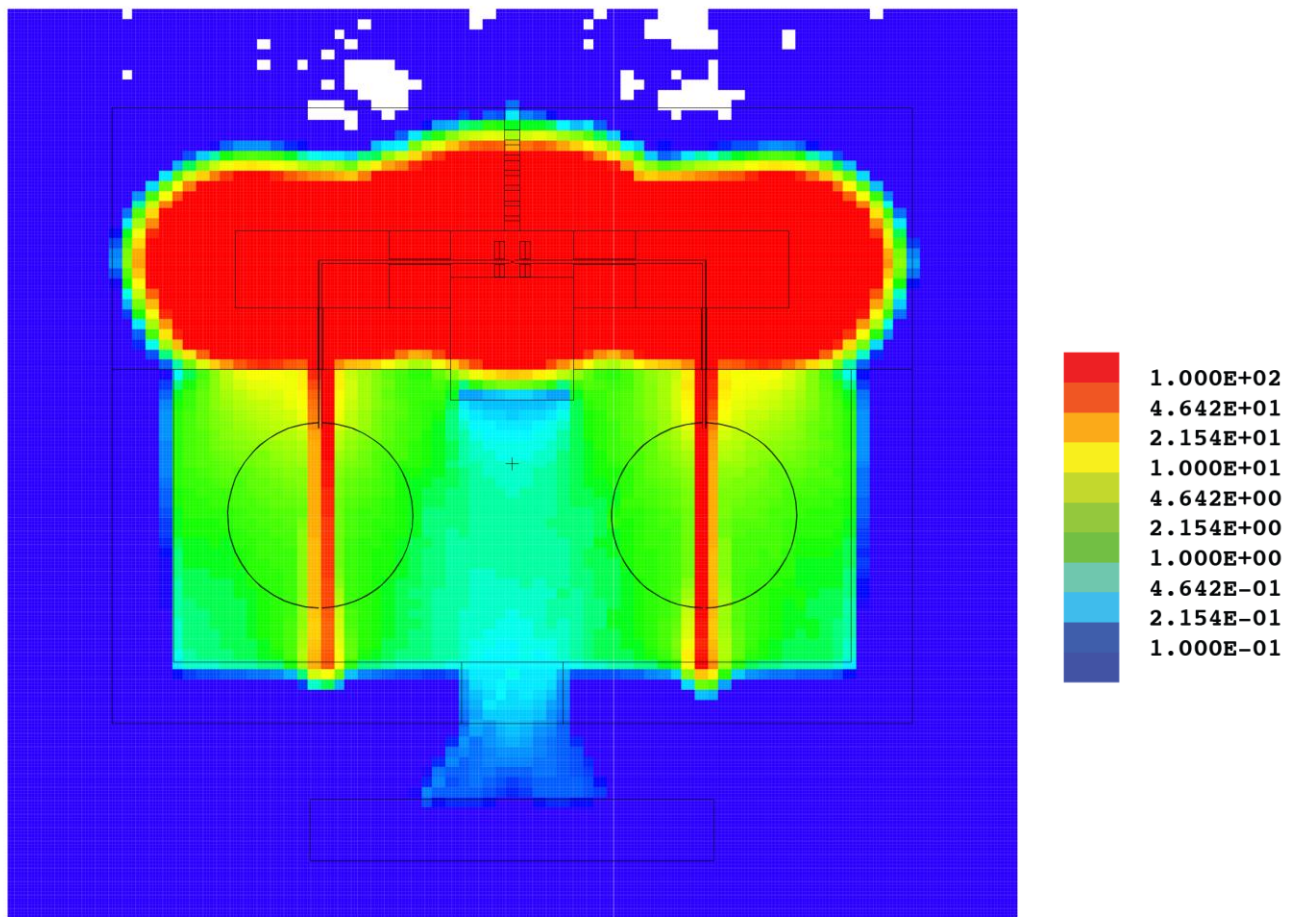


Figure 4. A second analysis, showing the beam pipe streaming through the shield wall.

### Horizontal Insertion of Targets

Another impact of the facility layout change is horizontal insertion of the target. That scheme is shown in Figure 5. The target is suspended on the end of a stalk up to 12 feet long made of steel. The steel does not necessarily run the entire length as a solid rod, but must be solid over sufficient length to shield neutrons. Some lead may also be added for gamma. This rod is extracted into and through a hot cell each time the target is replaced. This target stalk is centered in a larger 10 inch diameter pipe, which in turn is inside a 12 inch diameter pipe that contains the beam pipe vacuum. The helium lines run through the 10 inch pipe. These pipes must have either steps or bends to prevent radiation streaming, and must be loaded with sufficient shielding to protect personnel. For vertical insertion this is relatively straight forward, with all the loads in line with gravity. Horizontal insertion analysis will be performed in FY19 after detailed shielding analysis is done for this insert and the facility shielding scheme (high density or low density concrete) is determined.



stress. The pulsed beam imposes an oscillating thermal stress, which is considered a secondary stress. Secondary stresses are weighted differently in pressure vessel analysis, but are equally weighted with primary stresses when calculating an equivalent stress. Based on equivalent stress analysis, the target life is likely limited to 1 year or less. Any valid experimental evaluation would be most useful to the prediction of target window life.

## Appendix 1. Report in the Fatigue Analysis of the Target in the Rhodotron Pulsed Beam

Northstar has elected to use rhodotrons rather than linear accelerators to deliver the electron beam to their targets. This decision has imposed a much lower frequency beam pulse on the target, resulting in short duration high power deposition. The impact on the target window is of particular importance.

The target is a stack of Mo100 disks 0.5 mm thick and 29 mm in diameter, separated by 0.25 mm coolant gaps. There is a beam entry window on each side of the stack. There are 2 rhodotrons per target, each delivering nominally 120 kW to each side of the target. The target and target housing with windows are shown in Figure 1.

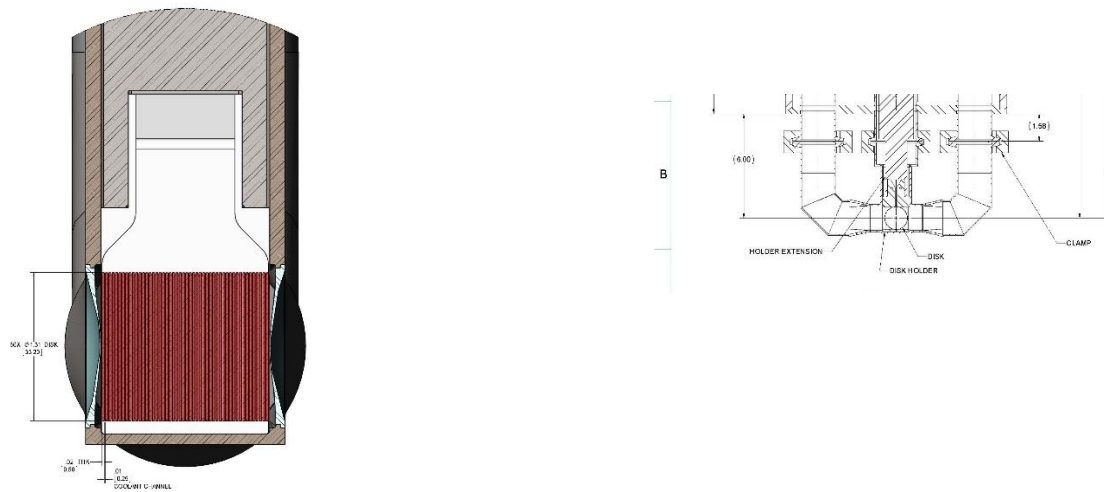


Figure 1. Target and target holder, with windows. In the view on the left, 2 beams will strike the target from each end, in the plane of the page. In the view on the right, the target is bottom center, the beam is into the page.

### Steady State Analysis

The steady state analysis of the target is reported elsewhere, but some summary is presented here for reference and completeness. The important performance parameters relevant to this pulsed beam analysis are the temperature of the window and the stress state at the operating pressure of 2068 kPa (300 psi). The beam heating profile is shown in Figure 2. The resulting target and window temperature are shown in Figure 3, with a peak window temperature near the center of 408°C.

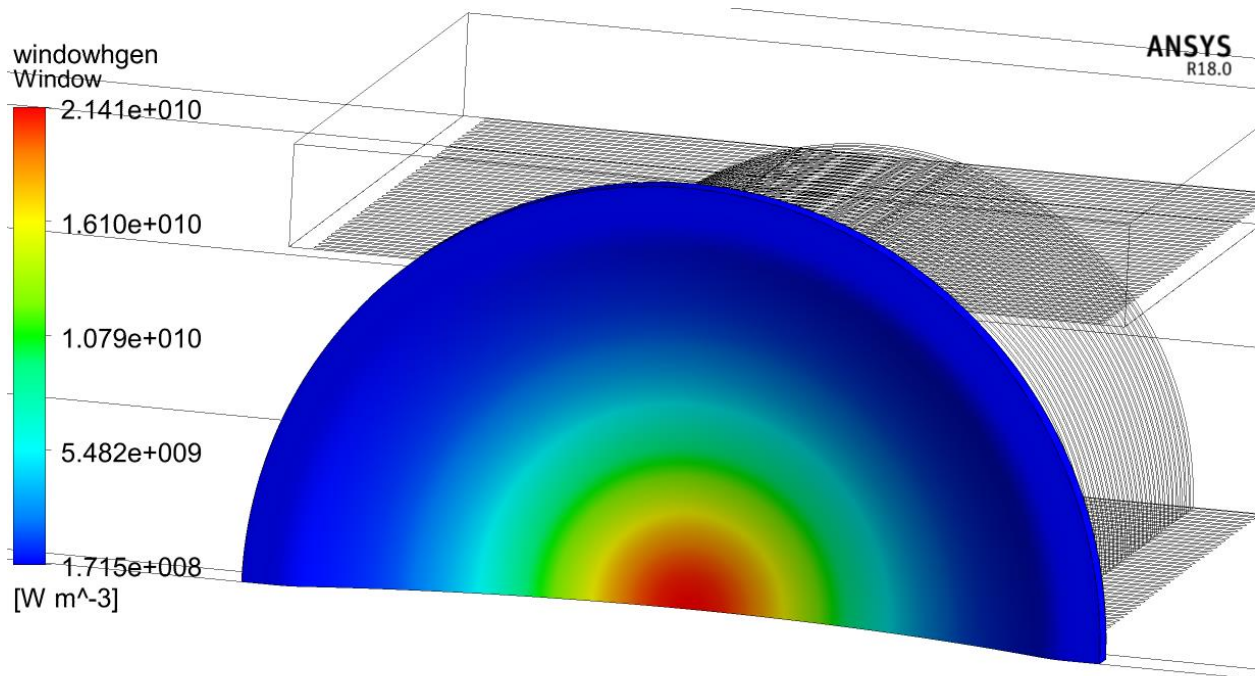


Figure 2. Window heat deposition.

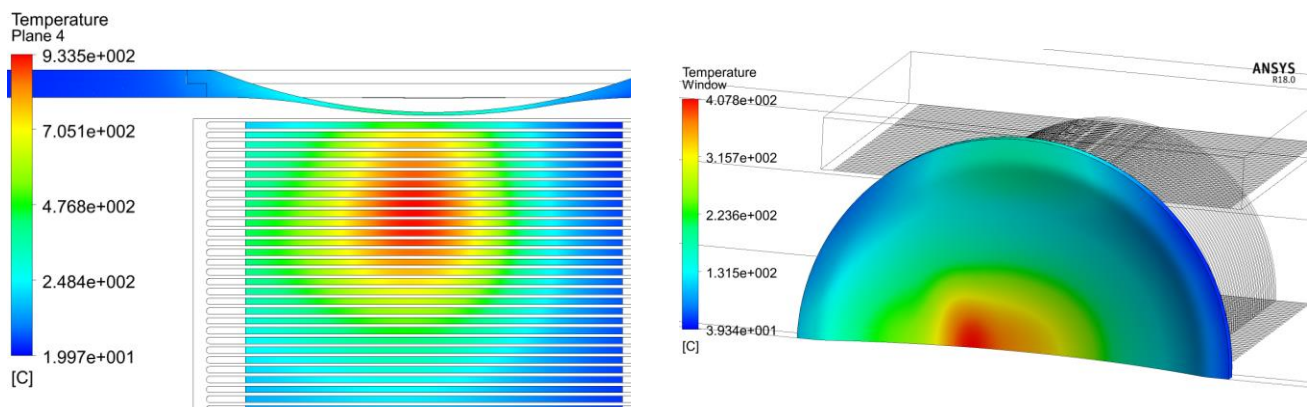


Figure 3. Temperature profiles in the target and the window.

The window is subjected to a primary mechanical stress (membrane plus bending) due to the pressure load, plus a secondary thermally induced stress. It is useful to consider these separately and in combination. The primary and primary plus secondary stresses are shown in Figure 4. The maximum primary stress is 258 MPa, peak combined primary plus secondary is 452 MPa.

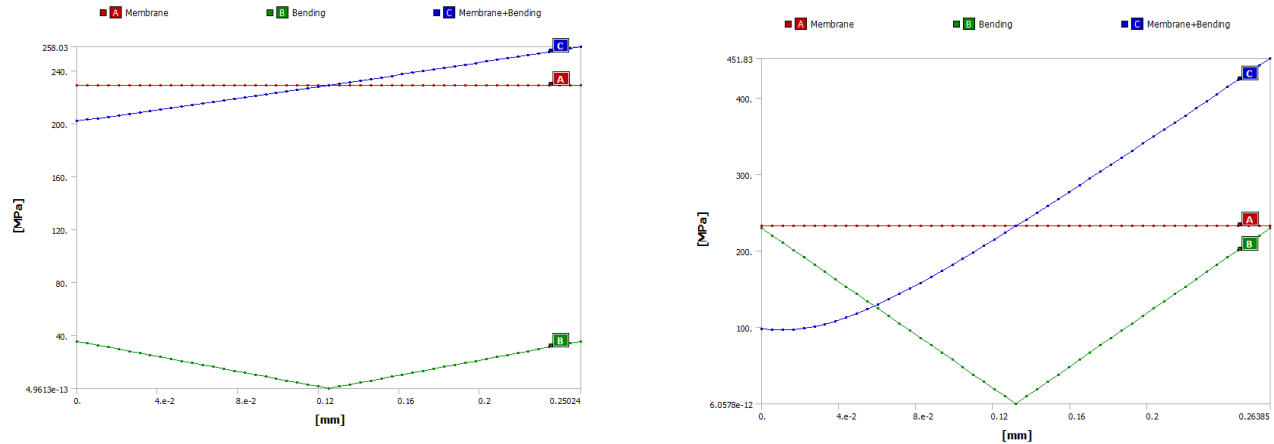


Figure 4. Primary and primary plus secondary stresses in the window.

### Pulsed Beam Transient Analysis

The pulsed beam currently measured at IBA is shown in Figure 5. The pulse is at 25 Hz with a 5 ms pulse width. The transient temperature response is shown in Figure 6. There is a nominally 200°C temperature oscillation with each pulse.

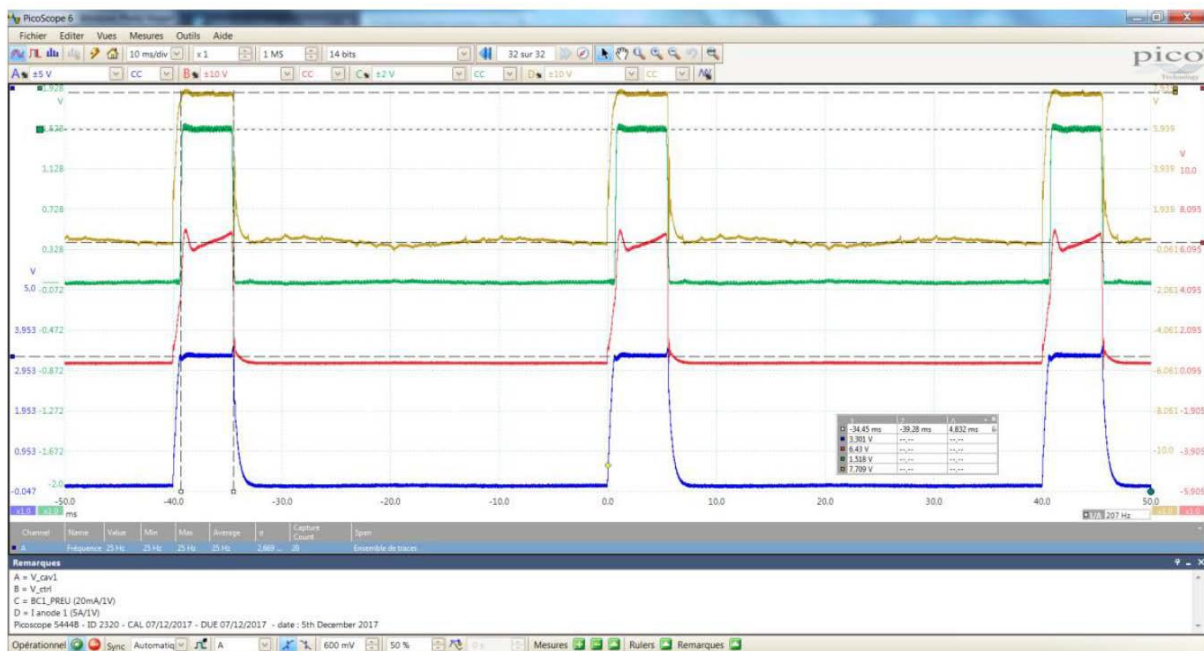


Figure 5. Pulsed beam structure, as of May 2018. Blue is voltage, green is current. The pulse is 5 ms at 25 Hz, of 12.5% duty factor.

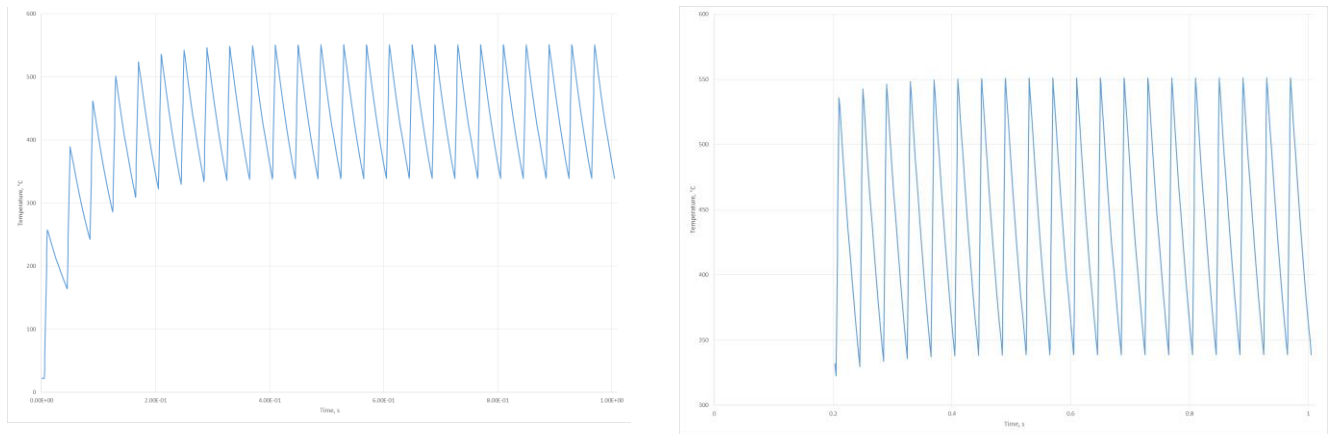


Figure 6. Pulsed beam temperature response.

## Fatigue

At 25 Hz and operating 6.5 days per week, 52 weeks per year, the window will be subjected to  $1.75 \times 10^9$  cycles. Fatigue curves for a given material at a given temperature are generally expressed as number of cycles to failure vs equivalent stress. In our case, the equivalent stress is 452 MPa at 550°C, the peak temperature during the pulse. This is a conservative measure of equivalent stress because of the large secondary stress contributor. However, it is the thermal stress that is cycling, the mechanical primary stress is a static applied stress invariant with time. There are no available similar load cases found in the literature.

Specialty Metals is the supplier for the Inconel 718 used in the window. In their material data sheet ([http://www.specialmetals.com/assets/smc/documents/inconel\\_alloy\\_718.pdf](http://www.specialmetals.com/assets/smc/documents/inconel_alloy_718.pdf)), on pp 17, they list fatigue strength at  $10^8$  cycles and 1000°F (537°C) as 90 ksi (620 MPa). As fatigue curves tend to approach an isotope, as will be seen below, and since 620 MPa is much greater than the window equivalent stress, no failure due to the pulsed beam can be expected based on this referenced data.

Kyle Buchholz, U. of Florida, did a study “High-Cycles Fatigue of Inconel 718” ([https://nationalmaglab.org/images/education/searchable\\_docs/college\\_early\\_career/reu/2017/buchholz.pdf](https://nationalmaglab.org/images/education/searchable_docs/college_early_career/reu/2017/buchholz.pdf)). The plot of that data, along with data from 3 other sources, is shown in Figure 7. This shows approaching a minimum of 500 MPa or greater at about  $2 \times 10^6$  cycles. This is also encouraging data in support of window life beyond one year.

Another fatigue curve from “Atlas of Fatigue Curves,” American Society for Materials, H. E. Boyer, 1986, is shown in Figure 8. In this data, the fatigue life has reached an asymptote at  $10^8$  cycles corresponding to 538°C and 420 MPa. This is much lower than the Specialty Metals data, and roughly equivalent to the Northstar window condition.

Strain range is another parameter besides equivalent stress for evaluation fatigue life. Calculated strain for the Northstar window at the maximum and minimum temperatures during the pulse are shown in Figure 9. Strain range, in percent, is 17. Figure 10 shows fatigue life as a function of strain range (AFCI Material Handbook, Rev. 5, LA-CP-06-0904). By this curve and this criteria, the target is likely to fail on very early. It should be noted that it is generally accepted that thermal fatigue is strain controlled, whereas mechanical fatigue is stress controlled (“Thermal Fatigue of Metals,” A Weronksi and T.

Hejwowski, Marcel Dekker, Inc, 1991). Having said that, the source of Figure 9 states “The investigators observed no apparent strain rate effects in the elastic regime.” The target window is well within the elastic regime. Hence, while the possibility of early failure due to strain range should not be discounted completely, it is not likely to cause failure. Further, the expected operating frequency will be 50 Hz with the same duty cycle. The temperature oscillations will be closer to 100°C, with strain range similarly reduced.

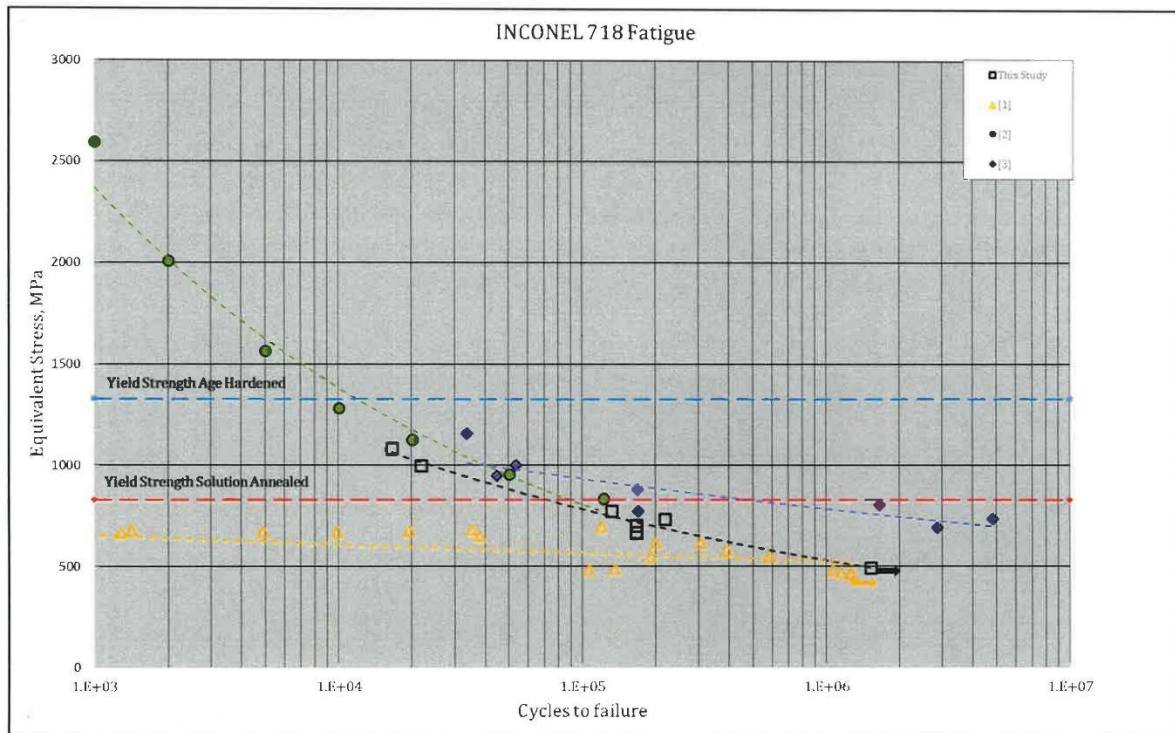


Figure 7. Inconel fatigue data from K. Buchholz, reference above.

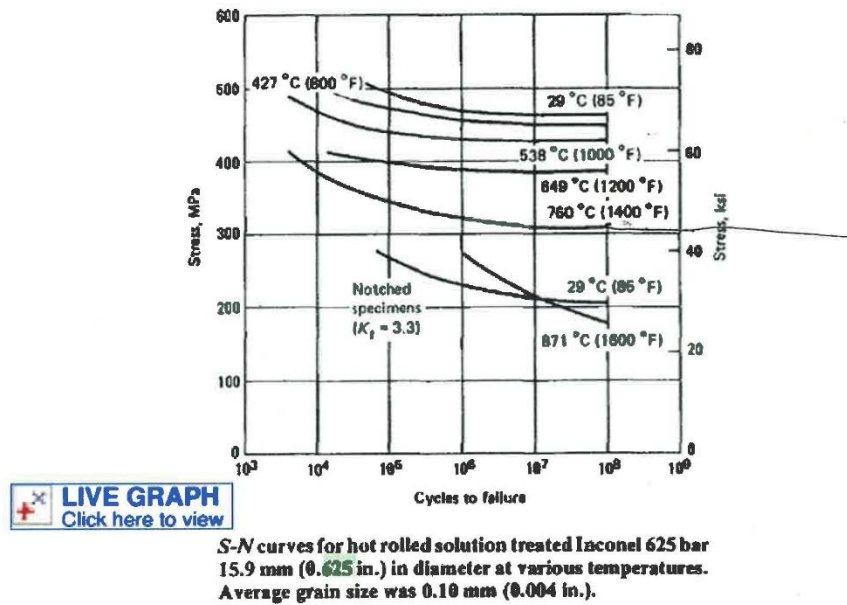


Figure 8. Fatigue curve for Inconel 718 from “Atlas of Fatigue Curves.” In this curve, the fatigue life at 538 C is about 420 MPa.

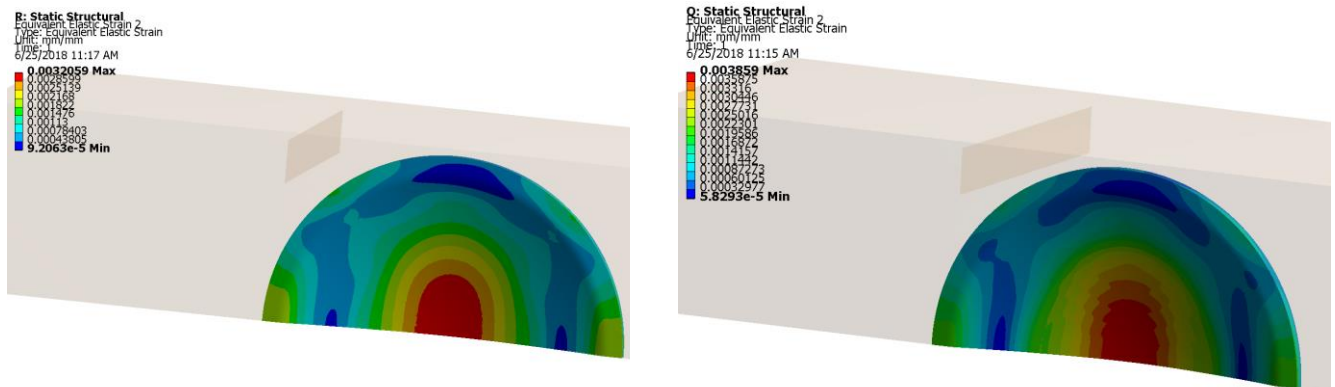
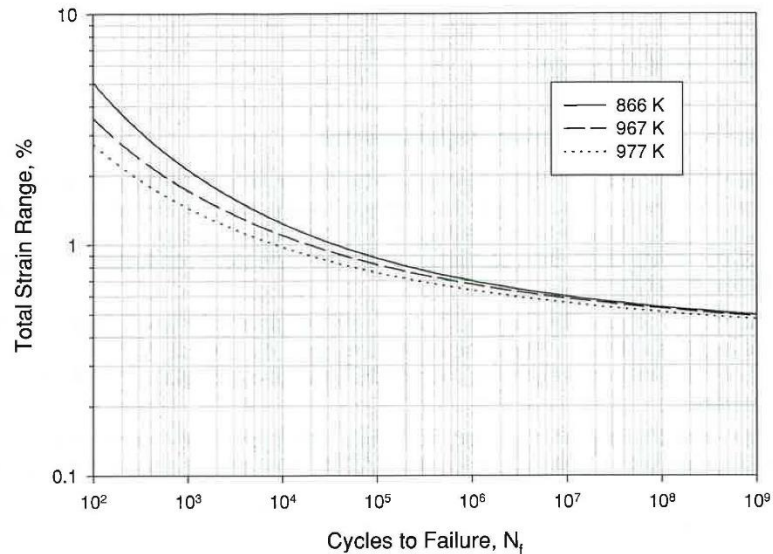


Figure 9. Northstar window strain at the extremes of the pulsed heating. Strain at target center is .0032 at 338°C (left) and .0039 at 550°C (left).



**Figure 2-40. S-N curves for fatigue of Alloy 718 for temperatures of 866 K, 922 K, and 977 K.**

Figure 10. Fatigue life of Inconel 718 based on strain range.

### Conclusion

The most important conclusion is that the fatigue life of the Northstar window, with its time invariant mechanical load and a superimposed cyclic thermal load, has no close parallel in the literature. Also, the equivalent stress curves referenced herein are not mutually consistent. There are too many variables in material condition for a direct comparison with published data. Further, while the target stress is well within the elastic regime, the strain range is high, so that criteria for fatigue life cannot be completely discounted. So, while available data suggests that the window can survive  $10^9$  cycles (1 year), the possibility of premature failure cannot be ignored. An experimental replication of the pulse strength and duration is highly recommended.

A pulse frequency increase from 25 to 50 Hz is expected. This significantly reduces the thermal oscillations and strain range concerns but uncertainty in predicting fatigue life remains.